

# Flat top optical multicarrier generation for ultra dense asymmetrical radio over fiber system

HARMINDER KAUR<sup>1,\*</sup>, MANJIT SINGH BHAMRAH<sup>1</sup>, BALJEET KAUR<sup>2</sup>

<sup>1</sup>*Electronics and Communication, Punjabi University Patiala, India*

<sup>2</sup>*Electronics and Communication, Guru Nanak Dev Engineering College, Ludhiana, India*

For the generation of the maximum number of tones with a high tone to noise ratio (TNR) and the lowest amplitude difference (AD), different optical multi carrier-generation (OMCG) configurations are investigated in presented work by incorporating amplitude modulators (AM), dual drive Mach-Zehnder modulators (DD-MZM), and phase modulators (PM). Three modulators are employed in each OMCG, and a total of twelve different arrangements are investigated, such as (i) AM-DD-MZM<sub>1,2</sub>, (ii) AM-DD-MZM-AM, (iii) PM-DD-MZM<sub>1,2</sub>, (iv) PM-DD-MZM-PM, (v) AM-DD-MZM-PM, (vi) PM-DD-MZM-AM in serial and (i) AM||DD-MZM<sub>1,2</sub>, (ii) AM||DD-MZM||AM, (iii) PM||DD-MZM<sub>1,2</sub>, (iv) PM||DD-MZM||PM, (v) AM||DD-MZM||PM, and (vi) PM||DD-MZM||AM in parallel. A single RF source is deployed in all the OMCG configurations, and no other fiber Bragg gratings (FBGs) or tailored methods are incorporated. Further, an asymmetrical ultra-dense high-capacity 70 km bi-directional Radio over fiber (RoF) system is presented by incorporating the proposed OMCG and transmitter diversity supporting 10 GHz RF signal.

(Received December 4, 2023; accepted June 5, 2024)

*Keywords:* OMCG, Tones, TNR, RoF, Transmitter diversity

## 1. Introduction

Throughout history, researchers have prioritized technological advancement in data transmission networks. More specifically, the need for more bandwidth-hungry applications is growing at a higher pace and accelerates the development and motivates scientists to create ultra-high capacity wireless and wired architectures [1-2]. The key attributes that are being focused on by the system designers during the commercialization of wireless/wired systems are high capacity, low cost, and improved performance [3]. In high-capacity multi-wavelength systems (also called wavelength division multiplexing (WDM)), where a large number of laser sources are required, the higher cost is a prevalent issue [4-5]. Nowadays, the use of WDM technology is becoming a mainstream technology in different optical communication applications such as RoF systems [6], Passive optical networks (PON) [7], Free space optical communication systems (FSOCS) [8], Inter-satellite optical wireless systems (IsOWCS) [9], and Visible light communication [10], etc. Optical multicarrier generation (OMCG) is the ultimate solution to address the constraints of high cost in the WDM system. Moreover, the optically flat OMCG with high TNR is a strong candidate for high-speed optical data transmission systems [11]. Different techniques have been explored in the literature for the realization of OMCG, such as (i) optical fiber nonlinearities-based supercontinuum generation [12], (ii) self-feedback oscillation [13], (iii) re-circulating frequency shifter (RFS) loop [14-16], and (iv) cascading of intensity/phase modulators [17-20] etc. The OMCG technique, which uses the nonlinearity of an optical medium such as in the super-

continuum generation, experiences temporal and spectral fluctuation and is therefore not an optimal solution for the flat multi-carrier generation [21]. In the aforementioned OMCG techniques, the phase shifters and optical filters have been incorporated in most of them but require high-powered RF signals through amplification except RFS loop [22]. In the RFS loop technique, the high-power RF amplifier is not required and therefore gets more attention from the researchers. However, the high noise emergence in each round trip of RFS loops forces designers to incorporate different noise-quelling techniques, which leads to high costs and more complexity [23]. The RFS loop exhibits high TNR, and a large number of carriers have been reported with either single-sideband or multi-sideband. It is perceived that the single-sideband modulation is more suitable for the RFS loop as compared to the multi-sideband modulation due to the generation of more optical comb lines. Amplitude spontaneous emission (ASE) affects the number of carriers in single-sideband modulation, and deployment of the optical finite impulse response (FIR) filters for ASE suppression ultimately increases the cost of the system [24-25]. Similarly, one of the prevailing technologies for OMCG is the cascading of diverse intensity modulators in different arrangements, such as using single drive (SD)/dual drive (DD) MZM with phase modulators [26-27]. For OMCG, the DD-MZM configuration has been investigated by incorporating a hybrid interferometer modulator but has some limitations such as fewer comb lines, a high AD, a high RF power amplifier, and costly components [28-29]. An OMCG based on the cascaded amplitude modulators is reported for 11 optical frequencies having AD < 2 dB [30]. A hybrid PM and polarization modulator arrangement are

presented in [31] for 32 optical carriers with AD 2.1 dB. Similarly, the DD-MZM-based configuration is proposed in [32] for 7 optical frequencies with AD < 1 dB. A total of 38 frequencies are generated by employing a PM and intensity modulator exhibiting AD~1 dB [33]. Literature review witnesses that AD increases with the increase in number of carriers. Therefore, flat optical tones are required for even transmission performance in WDM systems. Meanwhile, the immense use of bandwidth-hungry applications like video-on-demand, online gaming, and other multimedia applications introduces significant challenges to today's high-capacity, quick, and spectral-efficient optical networks. The need for effective systems that can handle high data rates will be what defines next-generation networks [39]. In the wireless domain, RF frequencies mitigate bandwidth shortening and spectrum congestion, whereas optical fiber offers a broad bandwidth and an extended communication range. RoF is used for wireless network traffic control and gives channel bandwidth access. Incorporating millimetre waves (MMW) into RoF systems makes them a possible contender for providing direct broadband wireless access to end users [40]. An OMCG-based RoF system employing a phase-modulated laser and two fiber bragg gratings was demonstrated in [41] for 7 comb lines and 40 dB TNR. A 10 Gbps RF-DD-MZM configuration generating 13 comb lines in an OMCG-RoF link was presented in [42] using 4-Quadrature amplitude modulation–orthogonal frequency division multiplexing (4-QAM-OFDM) over 50 km. Recently, two articles with OFMG using electro-absorption modulation were reported [43] [38], but their performance, as well as capacity, was limited due to high AD and a lesser number of tones. For the design of ultra-high-capacity next-generation WDM-RoF systems, with high cost-effectiveness, OMCG will be a potential candidate. The compact and cost-effectiveness network unit with less power management in the WDM-RoF system are the standout benefits of OMCG.

In this research article, a closely spaced tones based OMCG configurations are investigated by arranging the AM, DD-MZM and PM in serial as well as in parallel. The presented OMCG configuration is realized by three stages of modulators and being driven by single RF source for all modulators. It is noteworthy that the requirements of any specially tailored schemes and FBG are eliminated for flat top tones and DC biasing of the DD-MZM plays an important role in multi carrier generation and flat top tones in proposed work. Large number of tones can be generated with the incorporation of multiple stages of modulators and therefore, twelve different arrangements of modulators are investigated. Out of these investigated arrangements, maximum number of 1st order tones are generated in AM-DD-MZM1-AM based OMCG and offered least AD and highest TNR. Further, an ultra dense 10 GHz OMCG is incorporated in bi-directional asymmetrical RoF system using transmitter diversity. The following is a summary of the major contributions:

- In this work, multiple OMCG configurations are investigated incorporating AM, DD-MZM and PM for the first time as per the author's best knowledge.

- For OMCG, single RF source is used in both serial and parallel modulators arrangements and no FBG is incorporated.

- A detailed comparison of proposed OMCG is performed with the previously reported OMCG configurations.

- Deployment of OMCG in asymmetrical RoF system is performed for ultra dense, high capacity and cost-effective operations.

For the suppression of interference between downstream and upstream transmission, transmitter diversity is proposed.

The proposed research article is structured as: The principle of presented OMCG arrangements or configurations is discussed in Section 2, simulation design of serial/parallel OMCG and results are elaborated in Section 3. Investigation and results of asymmetrical RoF system is discussed in Section 4. Concluding remarks of presented OMCG and RoF system are briefed in Section 5.

## 2. Discussions and principles of OMCG arrangements

By supplying a high bandwidth for data transmission and engaging a large number of users in the network, the usage of OMCG benefits from a decrease in the number of laser sources at the signal generation side or the central office side. Various configurations of MZMs, PMs, and AMs are explored in serial as well as parallel to find the optimal configuration with high tone generation, high TNR and lowest AD. The output field of independent AM, DD-MZM and PM are expressed in equation (1-6), (7-9) and (10). The frequency of input laser signal is represented as  $f_0$ , initial phase is  $p_i$ , and amplitude is  $A_i$ . Probability density function for the laser noise is given as

$$f(\Delta p) = \frac{1}{2\pi\sqrt{\Delta f dt}} \cdot e^{-p^2/4\pi\Delta f dt} \quad (1)$$

where, time discretization is  $dt$ ,  $\Delta p$  is phase difference between two successive temporal instants and assumed Gaussian random variable, variance and zero mean is  $2\pi\Delta f$ , and laser linewidth is  $\Delta f$ . For  $n$  number of harmonics ( $n=0,1,2,\dots$ ), output  $A_{out}$  expression of AM incorporating RF signal i.e.  $f$  is represented as [36]:

$$A_{out} = |A_i| \sum_{n=-\infty}^{+\infty} A_{n,c} \cos[2\pi(f_0 + nf)t + p_{n,c}] \quad (2)$$

Phase and amplitude of  $n$  components is denoted by  $p_{n,c}$  and  $A_{n,c}$  respectively and their values can be calculated as expressed in equations (3) and (4) for phase and amplitude respectively.

$$p_{n,c} = [1 + n + (-1)^n \frac{\pi}{2} + np_1 + p_k] \quad (3)$$

where,  $p_k$  is the phase of the signal at  $k^{\text{th}}$  modulator,  $DC_{off}$  is DC offset, and peak to peak amplitude power is  $T_T$

$$A_{n,c} = \frac{1}{2} \left[ \cos(DC_{off} + n) \frac{\pi}{2} J_n \left( \frac{T_T \pi}{4} \right) \right] \quad (4)$$

Phase modulation on the input optical signal is performed by PM using electrical modulation and electrical input arm is driven by  $f$ . Laser output  $L_{out}$  is represented as

$$L_{out} = L_0 \cdot e^{j2\pi O_c t} \quad (5)$$

Carrier frequency is denoted by  $O_c$ , angular frequency is  $2\pi O_s$ , RF source output with respect to time  $f(t)$  is expressed as

$$f(t) = A \cdot \sin(2\pi O_s t + p_i) \quad (6)$$

Then output of the PM is  $L_{PMout}$  given as [44]

$$L_{PMout} = L_0 \cdot e^{j \cdot p_s \cdot f(t)} \quad (7)$$

Laser input to the PM is  $L_0$ ,  $f(t)$  is input RF signal,  $p_s$  phase induced by PM, and by putting the values of (5) and (6) in equation (7), we get

$$L_{PMout} =$$

$$L_{out} e^{j \cdot p_s \cdot f(t)} = L_0 \cdot e^{j2\pi O_c t} \cdot e^{j \cdot p_s \cdot A \cdot \sin(2\pi O_s t + p_i)} \quad (8)$$

Modulation index ( $m$ ) of the PM varied between 0 to 1 and final equation with Jacobi Anger expansion is [45]

$$L_{PMout} = L_{out} \sum_{-\infty}^{+\infty} J_n(\pi \cdot m) \cdot \exp(j2\pi(O_c + nO_s)t) \quad (9)$$

where, Bessel function is  $J_n(\pi \cdot m)$  of order  $n$  ( $n = \pm 1, \pm 2, \pm 3, \dots, \pm n$ ). Flat top comb lines can be generated with the deployment of MZM in serial or parallel configuration. Out of SD-MZM and DD-MZM, later one has more potential for more tones and lower AD. In equation (10), the output  $M_o(t)$  for DD-MZM including carrier and subcarriers for input  $M_i$ , RF frequency amplitudes for DD-MZM upper arm and lower arm are  $A_{f1}, A_{f2}$  respectively,  $V_{\pi RF}$  is switching voltage,  $V_{\pi DC}$  is switching bias voltage, DC bias voltages are  $V_{B1}, V_{B2}$  is given as [46]:

$$M_o(t) = \frac{1}{2} M_i e^{(jO_c t)} \left[ \sum_{-\infty}^{+\infty} J_n \left( \frac{\pi A_{f1}}{V_{\pi RF}} \right) \times e^{j \left( nO_c t + \frac{\pi}{V_{\pi DC}} V_{B1} \right)} + \sum_{-\infty}^{+\infty} J_n \left( \frac{\pi A_{f2}}{V_{\pi RF}} \right) \times e^{j \left( nO_c t + \frac{\pi}{V_{\pi DC}} V_{B2} \right)} \right] \quad (10)$$

In cascaded arrangements, output of first modulator is the treated as the carrier input of second and so on. However, in parallel arrangements, three individual outputs from modulators are combined and OMCG arrangements are evaluated in terms of TNR and AD.

### 3. Simulation design and results of OMCG configurations

Implementation of OMCG is accomplished in Optiwave's Optisystem by incorporating different modulators in serial and parallel. Further, results are evaluated in terms of TNR, number of carriers and AD.

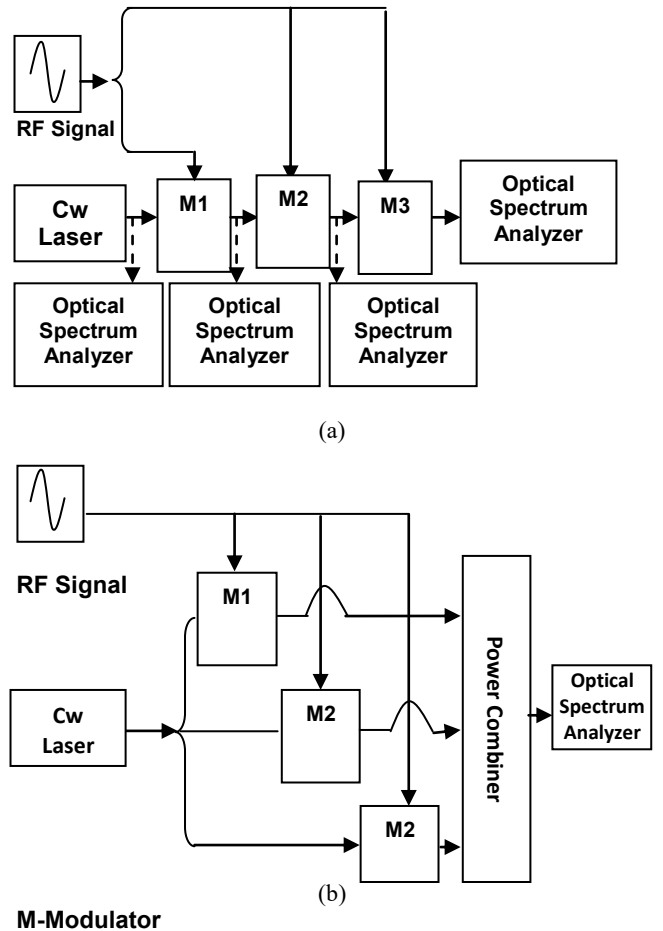


Fig. 1. Conceptual diagram for OMCG using modulators in (a) serial (b) parallel

The designs of different configurations of modulators such as AM, PM, and DD-MZM are proposed in serial as well as in parallel for obtaining the large number of carriers, high TNR, and flat top comb lines in OMCG. All the OMCG arrangements are proposed by keeping the  $f_0$  fixed at 192.15 THz, power at 15 dBm with 3 dB noise dynamics, and,  $\Delta f$  at 0.1 MHz. The time window for the proposed system is 1.28e-008 s, and the sampling rate ( $S_R$ ) is 6.4e+11 Hz. All the proposed configurations used only a

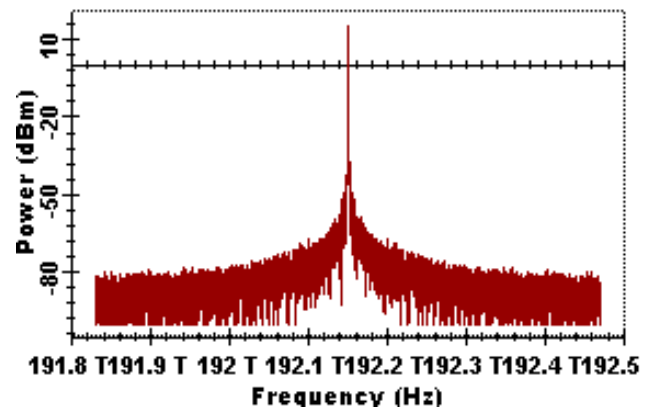
single 25 GHz RF signal (amplitude ( $f_A$ ) 5 a.u, bias ( $f_B$ ) 3 a.u) without any phase shifter and RF amplifier.

Table 1. Parameters and values of proposed OMCG modulators

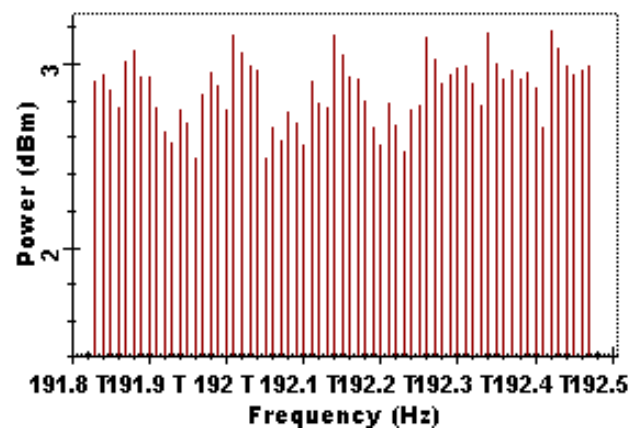
Parameters	Values
$f_0$	192.15 THz
$\Delta f$	0.1 MHz
$S_R$	6.4e+11 Hz
$p_i$	0
$f$	25 GHz
$f_A$	5 a.u.
$f_B$	3 a.u.
DD-MZM <sub>1,2</sub>	
$E_R$	40 dB
$V_{\pi RF}$	0.1 V
$V_{\pi DC}$	0.1 V
$V_{B1}$ and $V_{B2}$	20 V and 20 V
AM	
$m$	0.955
PM	
$p_s$	90 degrees

Total six different arrangements of three modulators in serial such as (i) AM-DD-MZM<sub>1,2</sub>, (ii) AM-DD-MZM-AM, (iii) PM-DD-MZM<sub>1,2</sub>, (iv) PM-DD-MZM-PM (v) AM-DD-MZM-PM (vi) PM-DD-MZM-AM are investigated and six in parallel are analyzed such as (i) AM||DD-MZM<sub>1,2</sub>, (ii) AM||DD-MZM||AM, (iii) PM||DD-MZM<sub>1,2</sub>, (iv) PM||DD-MZM||PM (v) AM||DD-MZM||PM (vi) PM||DD-MZM||AM. A conceptual diagram of the modulators placements in serial and parallel is illustrated in Fig. 1(a) and in Fig. 1 (b) respectively. Parameters of DD-MZM, AM, and PM modulators are kept constant during the simulation of serial and parallel configurations, and their values are displayed in Table 1. The values of  $m$  in AM,  $p_s$  in PM, and various DD-MZM parameters such as  $V_{\pi RF}$ ,  $V_{\pi DC}$ ,  $V_{B1}$ ,  $V_{B2}$ , and extinction ratio ( $E_R$ ) are cautiously chosen.

The output optical carrier spectrum of cw laser with weak sidebands and strong carrier is illustrated in Fig. 2 (a). In serial arrangements of modulators, there are total three cascaded modulators in each OMCG configuration and output spectrums are depicted in Fig. 2 (b), (c), (d), (e), (f) and (g) for AM-DD-MZM<sub>1,2</sub>, AM-DD-MZM-AM, PM-DD-MZM<sub>1,2</sub>, PM-DD-MZM-PM, AM-DD-MZM-PM, and PM-DD-MZM-AM.



(a)

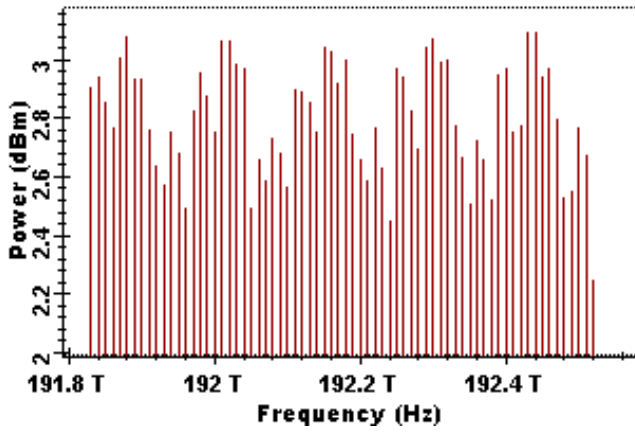


(b)

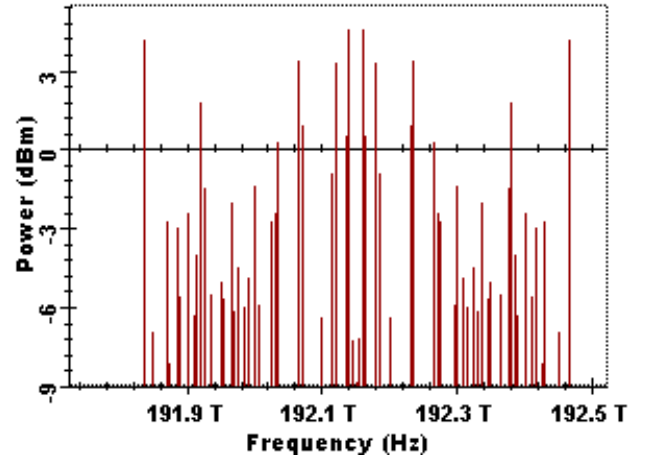
Fig. 2. Output carrier spectrum of (a) cw laser (b) after AM-DD-MZM<sub>1,2</sub>

### 3.1. Proposed OMCG using serial arrangements of modulators

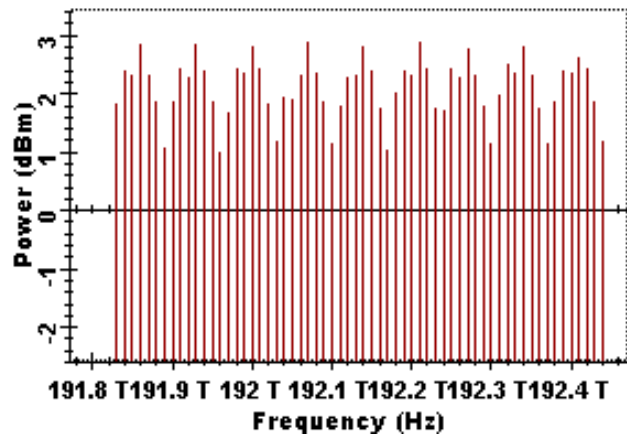
In AM-DD-MZM<sub>1,2</sub>, the drive of  $f = 25$  GHz is fed into AM and an energized output tones are obtained but these tones are not very much competent to carry modulated data. In order to stabilize the tones and to energize them further, DD-MZM<sub>1</sub> is placed after AM and it is described that more number of tones are generated and AD reduces significantly. However, more power is required for under energized sidebands and therefore, second stage of DD-MZM<sub>2</sub> is introduced for flat top tones followed by erbium doped fiber amplifier (EDFA) having gain 5 dB and noise Fig.4 dB. Optical carrier spectrum after DD-MZM<sub>2</sub> and EDFA is shown in Fig. 2 (b). In this OMCG configuration, 640 GHz bandwidth is covered by 65 total tones with 51.45 dB TNr and 0.66 dB AD. In second arrangement, DD-MZM<sub>2</sub> is replaced with AM and significant improvement in the tones is reported as illustrated in Fig. 2 (c). In AM-DD-MZM<sub>1</sub>-AM arrangement, we have received 690 GHz wide bandwidth and 71 flat top (AD=0.46 dB) tones with 52.58 dB TNr.



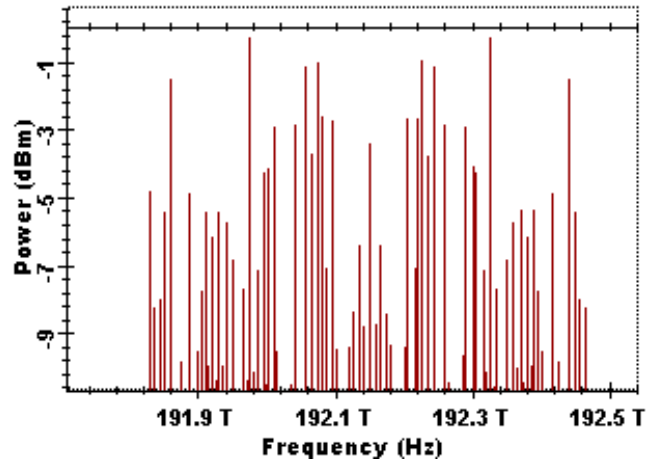
(c)



(e)



(d)

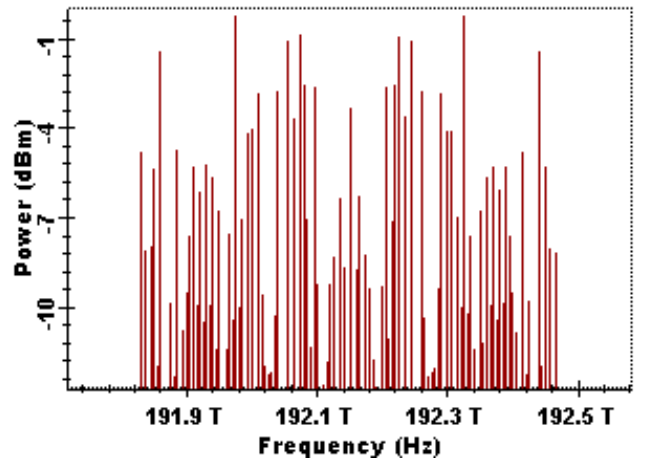


(f)

Fig. 2. Optical output tone spectrums of (c) AM-DD-MZM<sub>1</sub>-AM (d) PM-DD-MZM<sub>1,2</sub>

Further, a PM is cascaded with DD-MZM<sub>1,2</sub> and results revealed that output tones are reduced to 62 and bandwidth is restricted to 610 GHz only. Phase change led to the degradation in TNR (50.46) as compared to the two aforementioned OMCG configurations. Difference of amplitudes between the lowest energized and highest amplified tone is 1.86 dB as depicted in Fig. 2 (d). Next arrangement is PM-DD-MZM-PM and large AD has been seen and therefore divided into 1<sup>st</sup> order tones and 2<sup>nd</sup> order.

In the 1<sup>st</sup> order, total 14 tones are observed with 45.50 dB TNR and 4.08 dB AD followed by 2<sup>nd</sup> order tones with 16 tones and 4 dB AD as represented in Fig. 2 (e). Modulator diversity in cascaded modulators is accomplished by employing AM-DD-MZM-PM. A total of 14 tones are discerned for 1<sup>st</sup>-order with 46.69 TNR and 2.6 dB AD (Fig. 2 (f)). In 2<sup>nd</sup> order tones, a total of 21 tones are marked with 3 dB AD. Finally, in the last OMCG configuration, the first and final stage of cascaded modulators is swiped to form the PM-DD-MZM-AM arrangement. As shown in Fig. 2 (g), the number of first- and second-order tones noted is 18 and 24, respectively, and offered at 3.52 dB and 1.55 dB in the same order with TNR of 46.69 dB.



(g)

Fig. 2. Optical output tone spectrums of (e) PM-DD-MZM<sub>1</sub>-PM (f) AM-DD-MZM<sub>1</sub>-PM (g) PM-DD-MZM<sub>1</sub>-AM

### 3.2. Proposed OMCG using parallel arrangements of modulators

In different parallel arrangements of modulators, as mentioned before, only a single RF source is considered

and three parallel stages are taken into consideration for tones generation. Laser power is divided into three parts by deploying a power splitter and coupled to modulators. A power combiner is incorporated after modulation

operation to accumulate the output of all three modulators. Table 2 represents the output values of tones generated, TNR, and AD in parallel arrangements.

Table 2. Number of tones, TNR and AD values in parallel arrangement of modulators

OMCG configurations	Total no. of tones		TNR	AD
	1 <sup>st</sup> order	2 <sup>nd</sup> order		
AM  DD-MZM <sub>1,2</sub>	25	15	55.28	9.4 dB (1 <sup>st</sup> order) 2.01 dB (2 <sup>nd</sup> order)
PM  DD-MZM <sub>1,2</sub>	15	18	59.47	13.01 dB (1 <sup>st</sup> order) 1.9 dB (2 <sup>nd</sup> order)
AM  DD-MZM  AM	1	2	62.96	-- (1 <sup>st</sup> order) 0 dB (2 <sup>nd</sup> order)
PM  DD-MZM  PM	1	2	64.86	-- (1 <sup>st</sup> order) 0 dB (2 <sup>nd</sup> order)
AM  DD-MZM  PM	1	12	63.13	-- (1 <sup>st</sup> order) 5.7 dB (2 <sup>nd</sup> order)
PM  DD-MZM  AM	1	21	63.32	-- (1 <sup>st</sup> order) 12 dB (2 <sup>nd</sup> order)

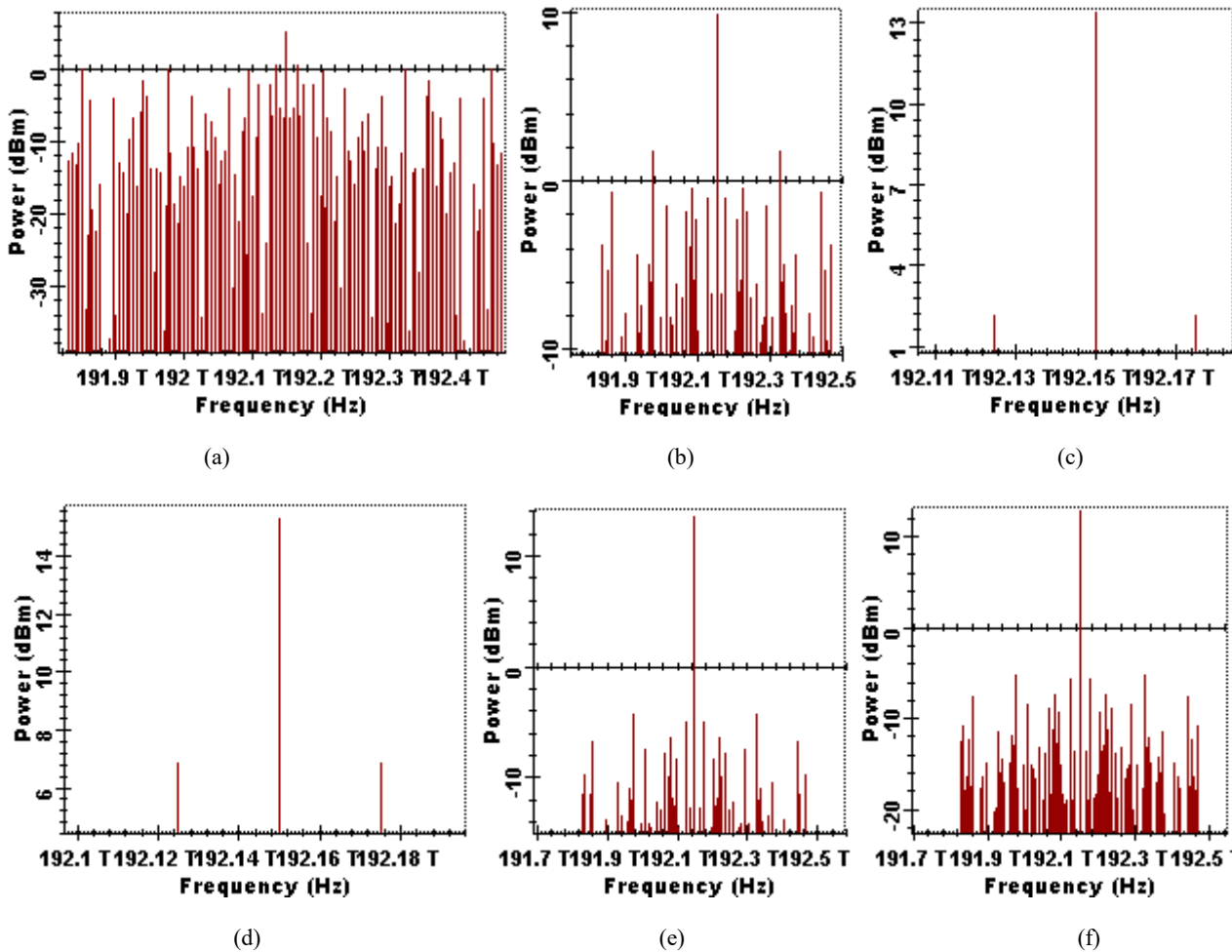


Fig. 3. Optical output tone spectrums of (a) AM||DD-MZM<sub>1,2</sub> (b) PM||DD-MZM<sub>1,2</sub> (c) AM||DD-MZM||AM (d) PM||DD-MZM||PM (e) AM||DD-MZM||PM (f) PM||DD-MZM||AM

Fig. 3 represents the total number of tones generated in different arrangements of modulators in parallel. It is evident that AM||DD-MZM<sub>1,2</sub> offered maximum 1st order tones (25) (2nd order 15) and 640 GHz bandwidth followed by PM||DD-MZM<sub>1,2</sub>, where 1st order tones are

15 and 2nd order is 18. Rest all the arrangements are inefficient to generate more than one tone of 1st order. The maximum number of 2nd order tones is observed in PM||DD-MZM||AM with 12 dB AD.

Table 3. Number of tones, TNR and AD values in parallel arrangement of modulators

OMCG configurations	Total no. of tones		TNR	AD
	1 <sup>st</sup> order	2 <sup>nd</sup> order		
AM  DD-MZM <sub>1,2</sub>	25	15	55.28	9.4 dB (1 <sup>st</sup> order) 2.01 dB (2 <sup>nd</sup> order)
PM  DD-MZM <sub>1,2</sub>	15	18	59.47	13.01 dB (1 <sup>st</sup> order) 1.9 dB (2 <sup>nd</sup> order)
AM  DD-MZM  AM	1	2	62.96	-- (1 <sup>st</sup> order) 0 dB (2 <sup>nd</sup> order)
PM  DD-MZM  PM	1	2	64.86	-- (1 <sup>st</sup> order) 0 dB (2 <sup>nd</sup> order)
AM  DD-MZM  PM	1	12	63.13	-- (1 <sup>st</sup> order) 5.7 dB (2 <sup>nd</sup> order)
PM  DD-MZM  AM	1	21	63.32	-- (1 <sup>st</sup> order) 12 dB (2 <sup>nd</sup> order)

### 3.3. Comparison of proposed OMCG with reported studies

A graphical comparison of different reported studies with proposed work in terms of TNR, number of tones, and AD is illustrated in Fig. 4 As discussed in Section 1, an efficient OMCG is decided based on three parameters

such as the number of tones, TNR, and AD. Under this condition, an optimal arrangement obtained is AM-DD-MZM1-AM due to a maximum bandwidth of 690 GHz, 71 flat top (AD=0.46 dB) tones, and the highest TNR of 52.58 dB. Table 4 shows the total OMCG lines, TNR and AD generated in different research works and in our proposed work.

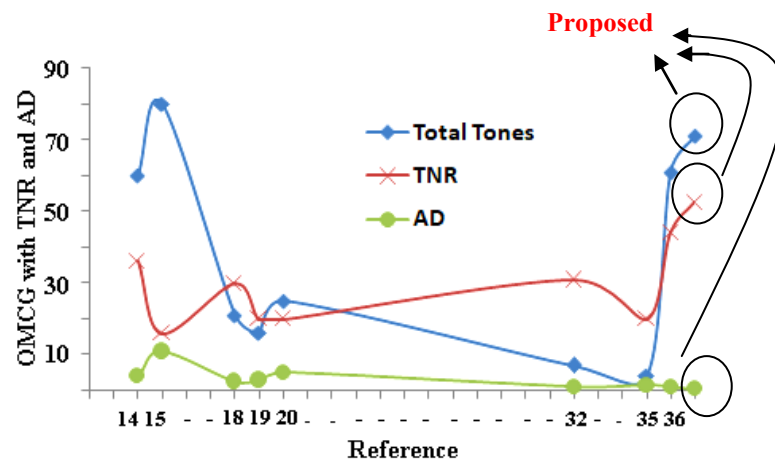


Fig. 4. Comparison of different reported studies and proposed work in cascaded configuration (color online)

Table 4. Comparison between various reported OMCG generation methods

Author [year] [Ref.]	Total OMCG lines at Data rate	TNR (dB)	AD (dB)	Technique
M. Fujiwara et al. [2001] [17]	256 at 1.25 Gbps	33.5	3	sinusoidal amplitude-phase hybrid modulation technique
M. Yamamoto, et al. [2005] [34]	29	-	5	Dual Frequency Optical Phase Modulation
T. Healy, et al. [2007] [30]	11 at 40 Gbps	-	1.9	two cascaded electro-optic polarisation modulators
R. Wu, et al. [2010] [33]	38	-	1	cascaded two phase modulators with third intensity modulator in series
J. Yu, et al. [2011] [18]	21 at 100 Gbps	30	2.5	cascaded two phase modulators with third intensity modulator in series
C. Chen, et al. [2013] [31]	13	-	2.1	cascaded polarization modulator (PoM) and phase modulator
J. Yu, et al. [2013] [19]	16	20	3	cascading one directly modulated laser and one phase modulator
Q. Wang, et al. [2014] [32]	7	31	1	SD-dual-parallel MZMs
X. Li, et al. [2015] [20]	25 at 112 Gbps	20	5	cascaded absorption modulated laser (EML) and one phase modulator
R. Ullah, et al. [2016] [35]	4 at 10 Gbps	20	1.5	laser source and phase modulator
X. Li, et al. [2017] [14]	60	36	4	three parallel MZM with RFS loop
J. Li, et al. [2017] [15]	80 at 10 Gbps	16	11	Dual-Polarization IQ Modulator Shared by Two Polarization-Orthogonal RFS loops
R. Ullah, et al. [2018] [36]	61	44	1	cascaded AM and two MZMs
B.Das, et al. [2020] [37]	54	-	0.5	parallel combination of four DD-MZMs
J. Yan, et al. [2021] [13]	17	-	7.7	phase-modulator-based dual-loop optoelectronic oscillator
V. Sharma, et al. [2022] [38]	24	-	1.1	two cascaded intensity modulators and a phase modulator
Proposed Work	71	52.58	0.46	three cascaded serial AM-DD-MZM-AM

#### 4. Operational Investigation of OMCG in asymmetrical WDM-RoF using MDRZ/CSRZ

A state-of-the-art OMCG-based optical line terminal (OLT) in asymmetrical 355 Gbps downstream and 5 Gbps

upstream WDM-RoF system is presented by incorporating transmitter diversity.

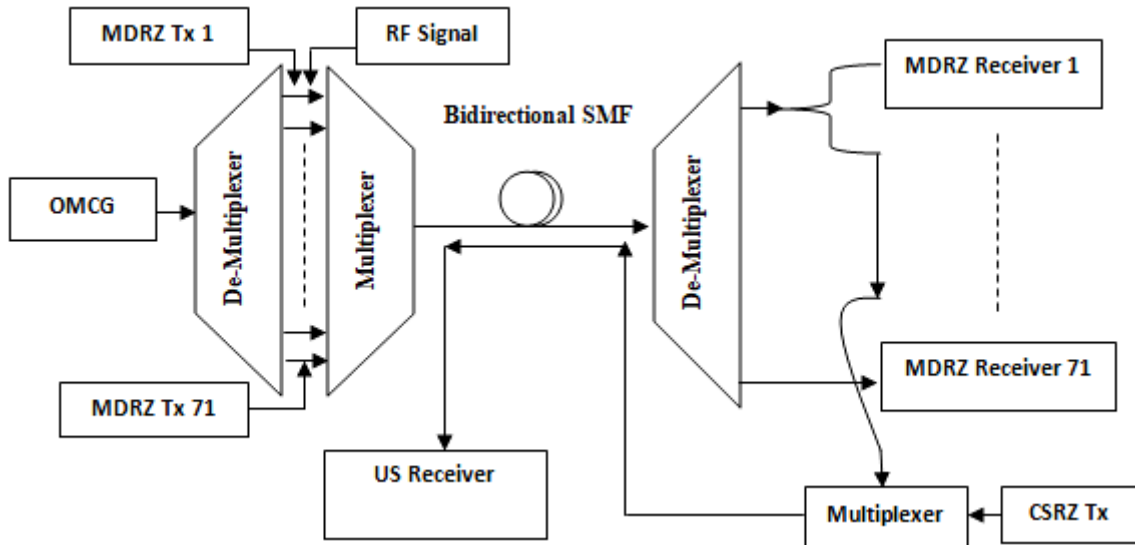
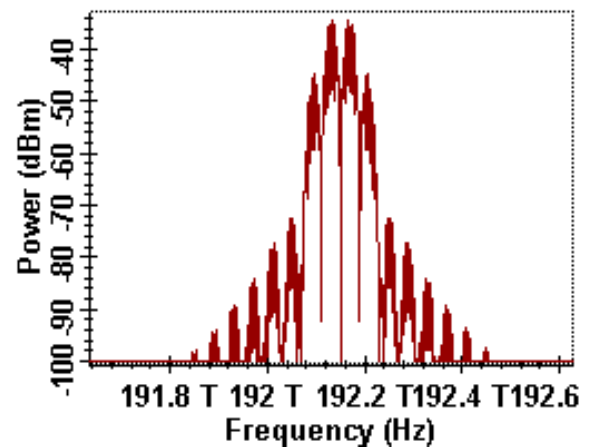
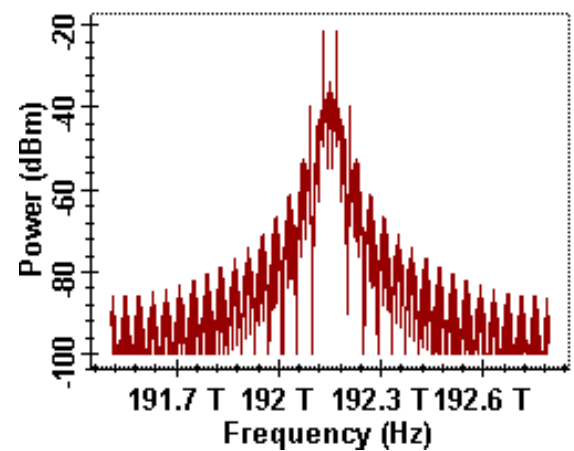


Fig. 5. Proposed asymmetrical RoF system employing OMCG and Transmitter diversity

For the OMCG in OLT, an optimal cascaded configuration, an AM-DD-MZM1-AM is incorporated for getting high capacity at a very low cost. In OLT, a total of 71 tones are generated at the channel spacing of 10 GHz and each channel carries 5 Gbps MDRZ modulated data as shown in Fig. 6 (a). All the modulated channels are further modulated with RF signal and amplified with 30 dB EDFA. Optical signal circulators are employed to differentiate upstream and downstream signals. Downstream RF-modulated signals entered through port 1 of the circulator and exited from port 2. The output of port 2 is coupled to bidirectional single-mode fiber (SMF) and finally reached to de-multiplexer at the receiver side. De-multiplexer routed the specific frequencies to the corresponding out port and followed by the photodetector, RF analyzer, low pass filter, 3R-regenerator, and BER analyzer. One-half of the first port is used for upstream transmission and modulated with CSRZ modulation (modulated spectrum shown in Fig. 6 (b)). The upstream signal is communicated via bi-directional SMF and received through a circulator at the receiver. Transmitter diversity is considered to lower the interference between downstream and upstream data. Effects of input RF signals are investigated on output log BER as shown in Fig. 7, and it is observed that the least BER is observed for 10 GHz RF signal for both upstream and downstream.



(a)



(b)

Fig. 6. Representation of optical spectrum of (a) MDRZ in downstream and (b) CSRZ in upstream

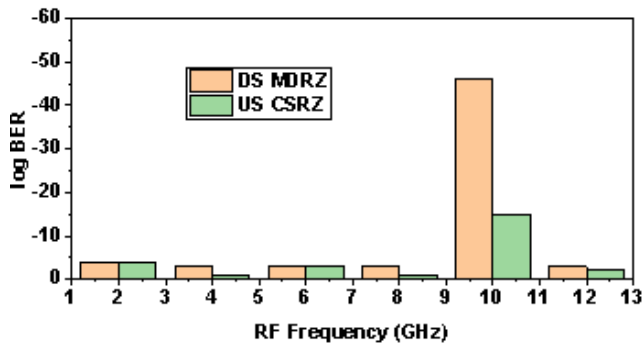


Fig. 7. Variation of log BER with input RF signal (color online)

To find the maximum supported distance in the proposed RoF system, the link length of bi-directional SMF is varied from 10 km to 90 km, and observations revealed that log BER increased with the link length enlargement in both downstream and upstream directions, as depicted in Fig. 8 (a). At the 70 km link length, the values of log BER downstream and upstream are -46 and -15, respectively. Beyond 70 km of distance, dispersion and attenuation, along with nonlinear effects, degrade the system's BER and push it out of acceptable limits ( $10^{-9}$ ).

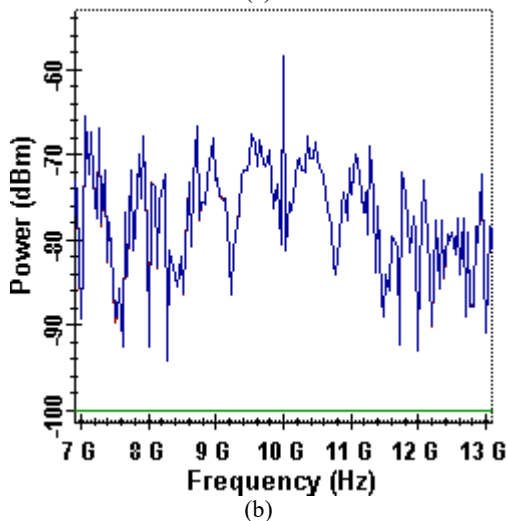
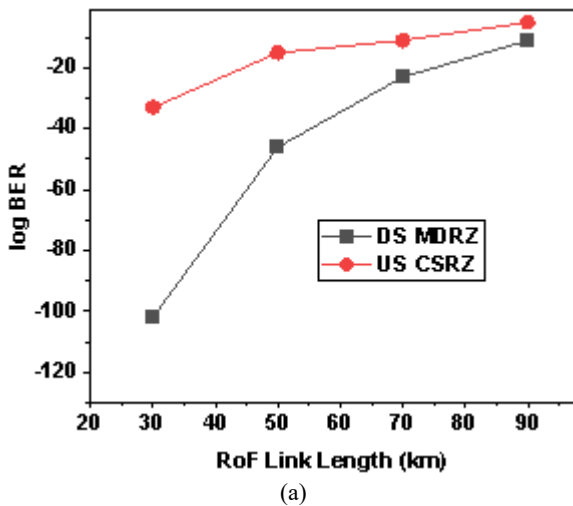


Fig. 8. Performance of proposed RoF system in terms of (a) log BER at different RoF link lengths and (b) RF spectrum

Upstream performance suffered compared to downstream because the upstream signal traveled twice as far as the downstream signal. Fig. 8 (b) represents the RF spectrum received downstream, and results disclosed that RF power -58.4 dB is received after a 70 km SMF link.

The eye diagram is the decision-end component for performance evaluation in terms of BER, Q factor, received power, eye-opening, eye closer penalty, eye height, jitter, etc. Fig. 9 illustrates the eye diagrams of the proposed asymmetrical RoF system at different link lengths, such as downstream eye diagrams at distances of (a) 10 km (b) 70 km (c) 90 km and upstream at (d) 10 km (e) 70 km (f) 90 km. Eye-opening is more in case 10 km in both upstream and downstream. However, in both cases, the maximum eye distance is 90 km. The downstream signal remains within the acceptable Q factor limit, i.e., 6 to 90 km; however, the upstream system can work only for 70 km.

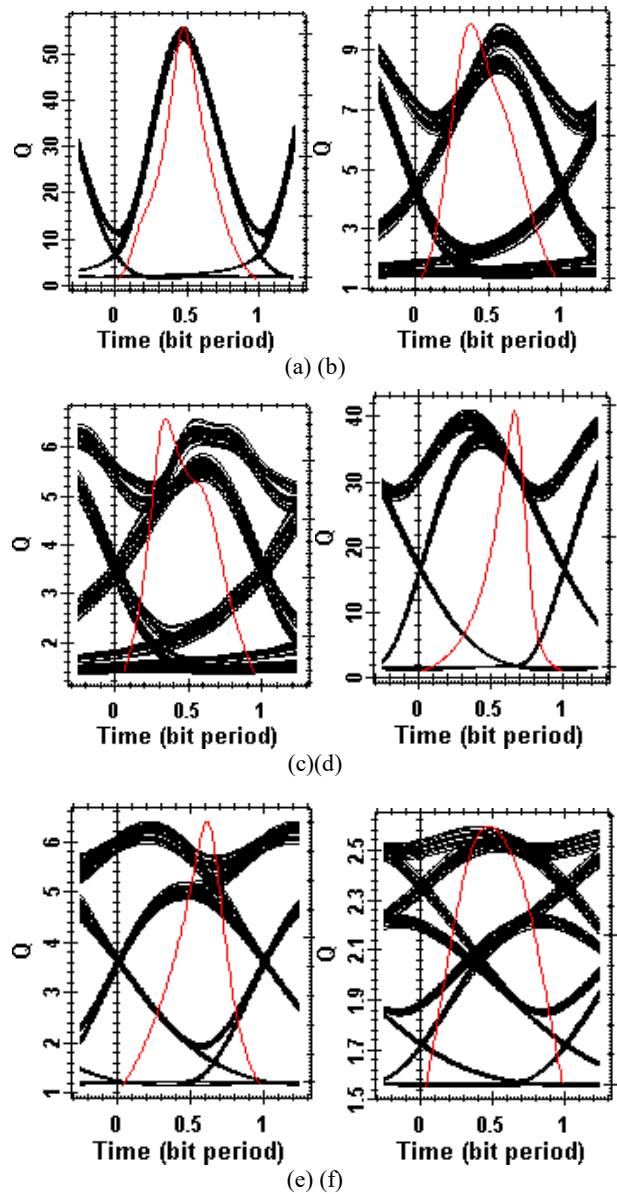


Fig. 9. Eye diagrams in downstream at (a) 10 km (b) 70 km (c) 90 km and in upstream (d) 10 km (e) 70 km (f) 90 km

## 5. Conclusion

We have presented two different operations in this research, such as (1) investigation of multiple OMCG configurations by using AM, DD-MZM, and PM modulators, and (2) demonstration of an ultra-dense and high capacity asymmetrical RoF system incorporating OMCG and transmitter diversity. Three-stage modulator arrangements are explored in serial and parallel to find an optimal OMCG configuration that can offer wide bandwidth through a large number of tones with high TNR and the least AD. Results revealed that the AM-DD-MZM1-AM arrangement had a maximum bandwidth of 690 GHz, 71 flat-top ( $AD=0.46$  dB) tones, and the highest TNR of 52.58 dB. In parallel arrangements, AM||DD-MZM<sub>1,2</sub> has provided a maximum of 25 1st-order tones with bandwidths of 640 GHz. Rest all the parallel arrangements have not produced more than one tone of the first order. Therefore, an OMCG based on AM-DD-MZM1-AM arrangement is incorporated in an ultra-dense, asymmetrical, and diversity-enabled RoF system. Results revealed that the proposed RoF system successfully covered 70 km of link length in both downstream and upstream directions with log BER values of -23 and -11, respectively.

## Acknowledgement

Harminder Kaur performed the proposed investigation under the Guidance of Dr. Manjeet Singh Bhamrah (Professor) at Punjabi university Patiala, India and also mentored by Dr. Baljeet Kaur (Professor) at GNDEC, Ludhiana, India.

## References

- [1] A. Kaur, B. Kaur, K. Singh, *Optik* **134**, 287 (2017).
- [2] H. Kaur, M. S. Bhamrah, B. Kaur, *Journal of Optical Communications* **26**, 549 (2022).
- [3] A. Kaur, M. S. Bhamrah, A. Atieh, *Optical Fiber Technology* **52**, 1 (2019).
- [4] J. Kaur, B. Kaur, K. Singh, *Wireless Personal Communications* **94**, 793 (2017).
- [5] S. Kaur, A. Verma, *Proceedings of the 4th International Conference on Advances in Science & Technology (ICAST2021)*, Available at SSRN: <https://ssrn.com/abstract=3868998> or <http://dx.doi.org/10.2139/ssrn.3868998> (2021).
- [6] F. Ketii, S. M. S. Atroshey, J. A. Hamadamin, *International Conference on Computer Science and Software Engineering (CSASE)*, IEEE, Duhok, Iraq, 95 (2022).
- [7] S. Sachdeva, J. Malhotra, M. Kumar, *Opt. Quant. Electron.* **53**, 549 (2021).
- [8] S. Sachdeva, M. Sindhvani, *Journal of Optical Communications* **8**, 335 (2022).
- [9] M. H. Ghazi, A. W. Abdulwahhab, A. K. Abass, *Journal of Optics*, Springer 2024.
- [10] S. Kaur, M. Kumar, A. Verma, *Journal of Optical Communications* **43**, 379 (2022).
- [11] B. S. Vikram, R. Prakash, K.P. Nagarjun, A. Singh, S. K. Selvaraja, V. R. Supradeepa, *OSA Continuum* **3**, 2185 (2020).
- [12] B. S. Vikram, Roopa Prakash, K. P. Nagarjun, Ajay Singh, Shankar Kumar Selvaraja, V. R. Supradeepa, *Optical Society of America* **3**, 2185 (2020).
- [13] J. Yan, R. He, *19th International Conference on Optical Communications and Networks (ICOON)*, IEEE, Qufu, China, 1 (2021).
- [14] W. Jiang, S. Zhao, X. Li, Q. Tan, *Optical Review* **24**, 533 (2017).
- [15] J. Li, H. Ma, Z. Li, X. Zhang, *IEEE Photonics Journal* **9**, 1 (2017).
- [16] Feng Tian, Ruoceng Zhang, Rahat Ullah, Bingyan Wang, Qi Zhang, Qinghua Tian, Bo Liu, Yongjun Wang, Xiangju Xin, *Optics Communications* **445**, 222 (2019).
- [17] M. Fujiwara, J. Kani, H. Suzuki, K. Araya, M. Teshima, *Electronics Letters* **37**, 967 (2001).
- [18] J. Yu, Z. Dong, N. Chi, *IEEE Photonics Technol. Lett.* **23**, 1061 (2011).
- [19] J. Yu, X. Li, J. Yu, N. Chi, *Chin. Opt. Lett.* **11**, 110606 (2013).
- [20] X. Li, J. Xiao, *Opt. Fiber Technol.* **23**, 116 (2015).
- [21] H. Takara, *Optics & Photonics News* **13**, 48 (2002).
- [22] Z. J. Yu, J. C. Nan, Y. Shao, L. Tao, Y. Wang, X. Li, *J. Lightwave Tech.* **30**, 3938 (2012).
- [23] Z. J. Yu, J. C. Nan, Y. Shao, L. Tao, Y. Wang, X. Li, *IEEE Photonics Technol. Lett.* **24**, 1405 (2012).
- [24] J. Lin, L. Xi, J. Li, X. Zhang, X. Zhang, S. A. Niazi, *Optics Express* **22**(7), 7852 (2014).
- [25] J. Lin, L. Xi, J. Li, X. Zhang, X. Zhang, S. A. Niazi, *Optics Express* **22**(12), 14087 (2014).
- [26] X. Zhou, X. Zheng, H. Wen, H. Zhang, Y. Guo, B. Zhou, *Opt. Commun.* **284**, 3706 (2011).
- [27] T. Sakamoto, T. Kawanishi, M. Izutsu, *Electron. Lett.* **43**, 1039 (2007).
- [28] Q. Wang, L. Huo, Y. Xing, B. Zhou, *Opt. Lett.* **39**, 3050 (2014).
- [29] T. T. Tran, M. Song, D. Song, D. S. Seo, *Electronics Letters* **55**, 43 (2019).
- [30] T. Healy, F. C. G. Gunning, A. D. Ellis, J. D. Bull, *Optics Express* **15**, 2981 (2007).
- [31] C. Chen, C. He, D. Zhu, R. Guo, F. Zhang, S. Pan, *Opt. Lett.* **38**, 3137 (2013).
- [32] Q. Wang, L. Huo, Y. Xing, B. Zhou, *Opt. Lett.* **39**, 3050 (2014).
- [33] R. Wu, V. R. Supradeepa, C. M. Long, D. E. Leaird, A. M. Weiner, *Opt. Lett.* **35**, 3234 (2010).
- [34] M. Yamamoto, Y. Tanaka, T. Shioda, T. Kurokawa, K. Higuma, *Integrated Photonics Research and Applications/Nanophotonics for Information Systems*, Technical Digest (Optica Publishing Group), paper ITuF5 (2005).
- [35] R. Ullah, Q. Zhang, H. A. Khalid, K. A. Memon, *China Communications* **13**, 76 (2016).
- [36] R. Ullah, Q. Zhang, H. A. Khalid, K. A. Memon, *IEEE Access* **6**, 6183 (2018).
- [37] B. Das, N. K. Das, J. Chakrabarty, S. F. U. Farhad,

- A. K. S. Gupta, *Results in Physics* **17**, 1 (2020).
- [38] V. Sharma, S. Singh, Lovkesh, *Photon Netw. Commun.* **44**, 133 (2022).
- [39] B. Kaur, A. K. Sharma, V. Kapoor, *Optics and Photonics Journal* **3**, 163 (2013).
- [40] S. K. Jalal, R. Z. Y. Al-Maqdici, *Arab. J. Sci. Eng.* **48**, 7043 (2023).
- [41] Y. Kim, S. Doucet, M. E. M. Pasandi, S. L. Rochelle, *Optical Society of America* **16**, 1068 (2008).
- [42] G. Li, Z. Lin, X. Huang, J. Li, *Electronics* **8**, 1064 (2019).
- [43] P. Jiang, P. Lin, Y. Fan, *Front. Optoelectron.* **15**, 1 (2022).
- [44] S. Ullah, R. Ullah, Q. Zhang, H. A. Khalid, K. A. Memon, A. Khan, F. Tian, X. Xiangjun, *IEEE Access* **8**, 76692 (2020).
- [45] J. Zhang, Nan Chi, Jianjun Yu, Yufeng Shao, Jiangbo Zhu, Bo Huang, Li Tao, *Optics Express* **19**, 12891 (2011).
- [46] B. Dai, Z. Gao, X. Wang, H. Chen, N. Kataoka, N. Wada, *Journal of Lightwave Technology* **31**, 145 (2013).

---

\*Corresponding author: harminder12.hk@gmail.com